Eur Respir Rev 2006; 15: 101, 148–156
DOI: 10.1183/09059180.00010105

Quantitative morphology of compensatory lung growth

C.C.W. Hsia

ABSTRACT: Compensatory lung growth is defined by the absolute increases in the quantity of functioning lung tissue in response to injury and/or disease, leading to a positive impact on functional outcome. The pneumonectomy model is used as an example to illustrate the salient features of compensatory growth and the specific considerations in its morphological quantification, including techniques of sampling and analysis, resolution of ultrastructural details, selection of markers for measurement, and interpretation of results in the context of organ architecture and physiology. The potential for structure–function dissociation is described in the present article. The current paper will discuss the application of high-resolution computed tomography to noninvasively quantify regional anatomy as well as temporal evolution of lung growth.

KEYWORDS: Airway, diffusing capacity, high-resolution computed tomography, lung alveoli, morphometry, pneumonectomy

CORRESPONDENCE
Dept. of Internal Medicine, University of Texas Southwestern Medical Center
Dallas
TX 75390-9034
USA
Fax: 1 2146488027
E-mail: Connie.Hsia@utsouthwestern.edu

SUPPORT STATEMENT
This research was supported by National Institutes of Health grants R01 HL045716, HL040070, HL054060 and HL062873.

Understanding lung growth requires quantitative knowledge of the amounts of constitutive components of the lung, their anatomical characteristics and relationships needed to function. Normal lung growth consists of two broad processes, as follows. 1) Generation of additional gas exchange tissue and blood–gas interfaces, as well as the conducting airways and blood vessels that supply them; and 2) ongoing remodelling of existing components in order to optimise tissue architecture and facilitate gas exchange. During development, physical forces imposed on lung tissue by respiration and an enlarging ribcage are believed to signal the myriad of biochemical regulatory pathways that interact to sustain cellular lung growth. During this period, adding alveolar hypoxia or supplementing selected growth factors may provide additional stimuli to augment some aspects of normal growth [1]. After epiphyseal closure at somatic maturity, mechanical interactions between the lung and thorax diminish and lung growth also ceases so that the sizes of the lung and thorax are ultimately matched. Thereafter, lung growth is re-initiated only if signals of sufficient intensity are re-imposed. The present article summarises the salient features of compensatory lung growth, the quantitative analysis of its morphology and the interpretation of results.

WHAT IS "COMPENSATORY LUNG GROWTH"?

Compensatory lung growth denotes the re-initiation or acceleration of cellular activities in response to injury or disease that generates new functioning tissue components in order to mitigate the impairment brought on by injury or disease. This definition highlights the following key concepts. First, growth is distinct from remodelling. In the absence of an absolute increase in functioning lung tissue, the occurrence of a higher air content, capillary congestion, unfolding of existing surfaces or re-arrangement of structural components does not constitute compensatory lung growth. Secondly, increases in tissue components that do not enhance organ function, for example, inflammation, fibrosis and interstitial oedema, do not constitute compensatory lung growth. Thirdly, since compensatory growth incurs additional metabolic costs and alters existing architecture, anatomical distortion may develop, leading to structure–function trade-offs and incomplete normalisation of organ function.

PNEUMONECTOMY: A MODEL OF COMPENSATORY LUNG GROWTH

In most patchy or diffuse lung diseases, responses of the injured regions are not easily separated from those of the normal regions; inflammation and fibrosis can obscure growth of the remaining functioning units. In contrast, major lung resection by pneumonectomy mimics the loss of functioning lung units in chronic restrictive disease. Since the loss is known and reproducible, and the remaining lung is normal, compensatory responses can be readily quantified. There is an extensive body of literature on

European Respiratory Review
Print ISSN 0905-9180
Online ISSN 1600-0617

the physiological and structural compensation in small and large animal lungs using this model, summarised in [1–3]; physical forces acting on the remaining lung are believed to signal post-pneumonectomy adaptation, although alveolar hypoxia and various growth factors and hormones also modulate the response. Chronic alveolar hypoxia has also been reported as a model of compensatory alveolar growth in actively growing animals [1, 4–7].

Regardless of the aetiology of disease, lung function can be maintained to a significant extent without invoking new tissue growth. The burden of ventilation and blood flow shifts onto the remaining normal units, causing unfolding and/or distension of the remaining alveolar surfaces, recruitment and distension of remaining capillaries, and redistribution of erythrocyte flow. These dynamic adjustments collectively enhance utilisation of existing microvascular reserves and are capable of increasing the diffusing capacity of the remaining lung by 40–50% [8, 9]. For example, in patients who have lost one lung by pneumonectomy, average lung diffusing capacity measured at rest is only ~30% below normal [10]. As long as the remaining lung is relatively normal, this modest diffusion limitation is readily tolerated. Comparable diffusion impairment in well-trained adult dogs following left pneumonectomy (45% lung resection) elicits a budding alveolar cellular response but no overt growth of septal tissue [11, 12]. The remaining lung increases by nearly 80% in volume; alveolar capillaries are enlarged, as would be expected from an increased blood flow. Alveolar type II epithelial cells more than double in volume without a concurrent increase in the volume of other septal cells and matrix or gas exchange surface areas (fig. 1) [12]. Type II epithelial cells are the putative resident progenitor cells in the lung and are widely implicated in alveolar growth, function, maintenance and repair. During lung injury and recovery, type II cells increase in abundance [13]. Where these extra type II cells arise from remains unclear; possible sources include transformation of bone marrow-derived or resident embryonic stem cells [14, 15], trans-differentiation of type I epithelial cells [16] or replication of existing type II epithelial cells.

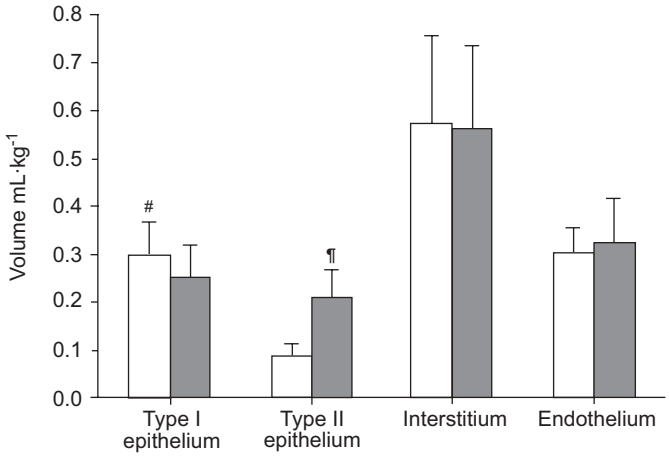

FIGURE 1. Volumes of alveolar septal tissue components were quantified in adult dog lung after left pneumonectomy (■) compared with the corresponding control lung (□). After left pneumonectomy there was a selective increase in type II epithelial cell volume. #: p=0.06; ¶: p<0.0001. Data are presented as mean±SD. Data are taken from [12].

In adult dogs, after more extensive resection of 55% of lung units by right pneumonectomy, the remaining microvascular reserves are fully utilised and limited growth of new alveolar tissue is initiated [17–19]. Post-pneumonectomy compensation is slow and incomplete in the adult lung [20, 21] but rapid and vigorous in the growing lung [22], an indication of the additive effects of developmental and post-pneumonectomy stimuli. In both young and adult dogs undergoing right pneumonectomy, alveolar septa in the remaining lung initially become thickened owing to a disproportionate increase in interstitial cells and matrix by nearly 3.6-fold, while epithelial and endothelial cells increase about two-fold compared with the control lung. Subsequently, the normal septal cell proportions are gradually restored with all cell types showing about a two-fold increase relative to age-matched control lungs, while the initial increase in gas exchange surface areas is maintained. As tissue remodelling or pruning returned the harmonic mean septal barrier thickness to normal, lung diffusing capacity also improves. These data broadly outline the sequence of events spanning several months during post-pneumonectomy compensation in large animal species. In comparison, in rodents, the time course of post-pneumonectomy lung growth is considerably shorter [23] and the intense cellular response heightens susceptibility to tumourigenesis as well as metastasis [24, 25]. It is probable that similar biochemical and molecular pathways are re-deployed during post-pneumonectomy alveolar growth as occurs during development, although in analysis by the present author's group of selected molecular pathways in the dog, compensatory growth does not exactly replicate developmental patterns of expression [26–28].

QUANTIFYING COMPENSATORY LUNG GROWTH

Technical considerations

Fixation

Quantifying lung growth typically requires invasive methods, such as instilling fixatives into the trachea at a constant airway pressure (0.18–0.25 kPa) under deep anaesthesia, resulting in a lung volume approximately halfway between functional residual capacity and total lung capacity. Owing to the elimination of surface forces, the instillation-fixed alveolar septa are completely unfolded, which is not a physiological state but allows for an estimation of the upper anatomical limit of alveolar surface area. An advantage of the instillation method is that pulmonary blood flow continues during the process, which allows fixation of capillary erythrocytes in a configuration more closely resembling the living state. The rate of progressive decline in pulmonary blood flow during instillation is not specifically controlled for, but is assumed to be similar among animals; the distribution of blood flow during fixation is also not controlled for, but is assumed to replicate the physiological state. In large lungs, it is possible that as the dependent regions are fixed first during the instillation procedure, the remaining pulmonary blood flow diverts to nondependent regions, resulting in greater capillary recruitment in nondependent regions. It is assumed that erythrocyte distribution in instillation-fixed lungs is similar to that in the basal living state.

An alternative method of fixation, by perfusion of fixatives into the pulmonary artery at a constant vascular pressure, has the advantage of preserving alveolar surface folds and lining fluid layer but has the disadvantage of removing the erythrocytes from blood vessels and capillaries [29]. With this method, it is possible to quantify alveolar cell volumes but not the blood–gas diffusion barrier. In addition, it is difficult to estimate the anatomical alveolar surface area, as the apparent surface area changes with the inflation state as well as the presence of surface lining fluid.

Sampling

Unbiased tissue sampling is a prerequisite of morphometric analysis and sampling methods must be selected according to the structures of interest. For example, assessing airway and vascular growth requires sampling procedures that specifically account for their anisotropic orientation; these methods are well described elsewhere [30, 31]. In assessing compensatory growth, a critical step is standardisation of the reference space, which ideally should be the volume of normal lung regions while the diseased regions are excluded. In the pneumonectomy model, standardisation is relatively easy. The remaining lung nearly doubles in volume; therefore, for comparison with the corresponding normal lung, about twice as many tissue blocks should be sampled and analysed from the post-pneumonectomy lung so that the sampling rate per unit of lung volume remains the same. Unbiased sampling is more difficult to achieve in diffuse or patchy lung diseases, where a global estimate, *e.g.* by computed tomographic scan, of the extent and distribution of normal and pathological regions may be necessary in order to quantify the reference space in which compensatory growth is expected to occur and direct tissue sampling to those regions.

Unbiased sampling should also account for the inherent heterogeneity in lung structure. Significant gravitational and nongravitational gradients normally exist in ventilation and perfusion, as well as in the corresponding airway and vascular anatomy [32, 33]. Interlobar heterogeneity becomes exaggerated as lung size increases. In dog lungs, the growth rate among lobes is uniform during post-natal development but non-uniform following pneumonectomy [34], an observation highlighting the need to sample and analyse each lobe separately in order to discern regional effects.

Analysis

Lung volume is the most basic and critical measurement as it defines the absolute reference space to which all estimates of volume and surface densities are referred. Lung volume is usually measured by saline immersion of the intact fixed lung or by point-counting using the Cavalieri principle after serial sectioning. As elastic fibres are incompletely fixed by glutaraldehyde, residual elastic recoil persists until tissue dehydration with ethanol [35, 36]. Even after release of airway pressure, lung volume measured by immersion is systematically higher than that by the Cavalieri method, especially in large lungs; the difference reflects refolding or crumpling of alveolar septa after the fixative is drained [36]. The Cavalieri method is preferred over the immersion method because the former yields a volume estimate that more precisely represents the relaxed state of the tissue being analysed under microscopy.

The alveolar–capillary cell volumes, surface areas and the diffusion barrier are measured using standard stereological techniques [37, 38]. The ultrastructural dimensions of the alveolar–capillary gas exchanger are best quantified under electron microscopy for several reasons, as follows. The composition of septal cells and matrix components cannot be adequately separated under light microscopy; a magnification of $\sim 1{,}000\times$ is required to reliably distinguish septal tissue from capillary blood and to detect surface irregularities. Without sufficient resolution it may be difficult to decide whether an apparently lower alveolar surface area is due to true loss of surface or greater folding of existing surfaces that could not be visualised at a low magnification. The accurate measurement of blood–gas barrier thickness requires a magnification of $\geqslant 8{,}000\times$. Magnification should be standardised across experimental groups because surface density, like the coastline, is a fractal quantity: its absolute magnitude increases with resolution.

Markers of alveolar growth

According to Fick's law, the major determinants of gas transport across alveolar membrane by diffusion are the surface area and harmonic mean thickness of the tissue–blood barrier, which is described by the following equation:

$$\text{Membrane conductance} = (k \cdot \text{surface area})/\text{barrier thickness} \quad (1)$$

where k is a permeability coefficient. While alveolar epithelial and endothelial surface areas increase with compensatory alveolar growth, these parameters do not describe dynamic surface interactions in the living lung where gas exchange across the tissue membrane must be matched to that across erythrocytes, which constitute the sink for oxygen uptake. In the fixed lung, total capillary erythrocyte membrane surface greatly exceeds alveolar or capillary surface area. However, erythrocytes deform in order to pass through alveolar capillaries; at a given moment in transit, only a fraction of the erythrocyte membrane interacts effectively with tissue membrane in gas uptake [39]. In addition, erythrocyte distribution is non-uniform, varying with capillary perfusion as well as with haematocrit (fig. 2). When observed under *in vivo* videomicroscopy *via* a transparent window through the chest wall, many subpleural capillaries are perfused predominantly by plasma with infrequent or no erythrocyte traffic at basal conditions [40]; these capillaries cannot effectively participate in gas exchange. As blood flow and pressure increase, erythrocyte traffic also increases [40], resulting in better tissue–erythrocyte matching and enhancement of gas uptake. Raising blood volume and haematocrit improves tissue–erythrocyte matching by increasing erythrocyte traffic through more capillaries and reducing inter-erythrocyte spacing [41–44]. Dynamic membrane interactions are difficult to quantify but are fundamental to microvascular function. For example, body mass-specific lung volume is similar between dog and human (50–60 $mL \cdot kg^{-1}$) and body mass-specific alveolar and capillary surface areas are only 30 and 13%, respectively, higher in the dog [17, 45]. Compared with the human, lung and membrane diffusing capacities increase faster with respect to pulmonary blood flow in the dog; peak membrane diffusing capacity is four-fold that in the average human and 2.6-fold that in the elite athlete [46]. Efficient

FIGURE 2. An electron micrograph from dog lung illustrates non-uniform distribution of erythrocytes within and among alveolar capillaries.

microvascular recruitment in the dog lung is largely explained by exercise-induced polycythaemia owing to a large spleen, which contracts upon sympathetic stimulation and injects ~10% of the total body erythrocyte mass into the circulation, thereby facilitating the utilisation of available tissue–capillary membrane for diffusion [47]. In the human, exercise-induced polycythaemia is limited, as is microvascular recruitment [46]. Thus, normal alveolar function is constrained not by anatomical tissue surfaces but rather by the magnitude and pattern of capillary erythrocyte traffic. In the presence of destructive lung disease, distension and growth of remaining capillaries provide compensation not only by increasing absolute tissue membrane surfaces and resident erythrocyte volume but also by optimising erythrocyte traffic to facilitate interactions at the tissue–blood interface.

A net increase in cell volume indexes cellular growth by hyperplasia and/or hypertrophy; these two processes can be distinguished if the number of nuclei of a given cell type is also estimated. Counting cell nuclei is a cumbersome task and the cell number is not a critical indicator of lung function; hence it is generally more expeditious to infer cellular growth from differential cell volumes rather than cell numbers. Another parameter commonly used in assessing lung growth is the number of alveoli. A larger number of alveoli indexes greater subdivision of the alveolar space but does not necessarily translate into a higher diffusing capacity of the blood–gas barrier unless alveolar–capillary surface area also increases and/or barrier resistance decreases. This potential dissociation between alveolar number and function is exemplified in the use of supplemental all-*trans*-retinoic acid to enhance post-natal alveolar septation. In rats treated with retinoic acid compared with placebo-treated control animals, the alveoli are smaller with more subdivisions, but surface area estimated under light microscopy is unchanged [48] and physiological lung diffusing capacity is not improved [49].

Alveolar capillary growth is associated with increased capillary blood volume, endothelial cell volume as well as surface area, and morphological evidence of capillary formation and/or subdivision. The developing lung typically exhibits double septal capillary profiles (fig. 3). With maturation the septum thins and lengthens, creating predominantly single septal capillary profiles with thin and thick sides of the diffusion barrier. The prevalence of double capillary profiles is normally quite low in adult dog lungs (2–3%) and about four-fold higher in growing lungs. During compensatory growth in the adult lung after right pneumonectomy, double capillaries are modestly elevated and the increase further accentuated following exogenous all-*trans*-retinoic acid supplementation [19]. In the absence of overt alveolar growth after left pneumonectomy in the adult lung, there is no increase in double capillary profiles. The reappearance of immature capillary morphology suggests neocapillary formation, perhaps by the growth of a tissue pillar into an existing capillary lumen eventually dividing it into two capillaries, a process termed ''intussusception'' [51], which has been observed in the developing lung.

After quantifying individual cell compartments, the next step is to consider their aggregate effects on organ architecture and function. Using all-*trans*-retinoic acid supplementation again as an example, its induction of post-natal and compensatory septal growth is associated with alveolar distortion (fig. 4). In addition to causing smaller airspaces in the normal growing lung (previously discussed), retinoic acid given to adult dogs after right pneumonectomy selectively enhances alveolar capillary formation and endothelial cell volume in the remaining lung without altering epithelial or interstitial volume, alveolar surface area or harmonic mean thickness of the diffusion barrier; the volume density and arithmetic mean thickness of the septum increase and alveolar surface/volume ratio actually declines [19]; the latter findings are consistent with altered septal geometry. From the alveolar–capillary surface area, the harmonic mean thickness of tissue–plasma barrier and the capillary blood volume, a morphometric lung diffusing capacity can be estimated [38, 52], which correlates reasonably with physiological diffusing capacity measured at peak exercise [53]. In retinoic acid-treated lungs, morphometric membrane and lung diffusing capacities are unchanged from those in placebo controls, while physiological diffusing capacities are either unchanged or reduced depending on the lung volume at which measurements are performed [54]. Therefore, retinoic acid administration fails to improve gas exchange despite selective enhancement of alveolar cellular growth. This example illustrates how non-uniform manipulation of a coordinated natural response could exert a positive impact on cell growth but a neutral-to-negative impact on organ function.

Markers of airway growth

In large mammals, the basic gas exchange unit, an acinus, contains several generations of gas exchange airways (respiratory bronchioles and alveolar ducts). Following pneumonectomy, respiratory bronchioles increase in absolute volume and number of branch points [18]; proliferation of respiratory bronchioles could occur either by transformation of the first generation of alveolar ducts into respiratory bronchioles or by alveolisation of the terminal bronchiole. Growth of acinar airways is proportional to that of alveolar tissue, a finding that should enhance compensation by improving intra-acinar gas conductance and mixing efficiency.

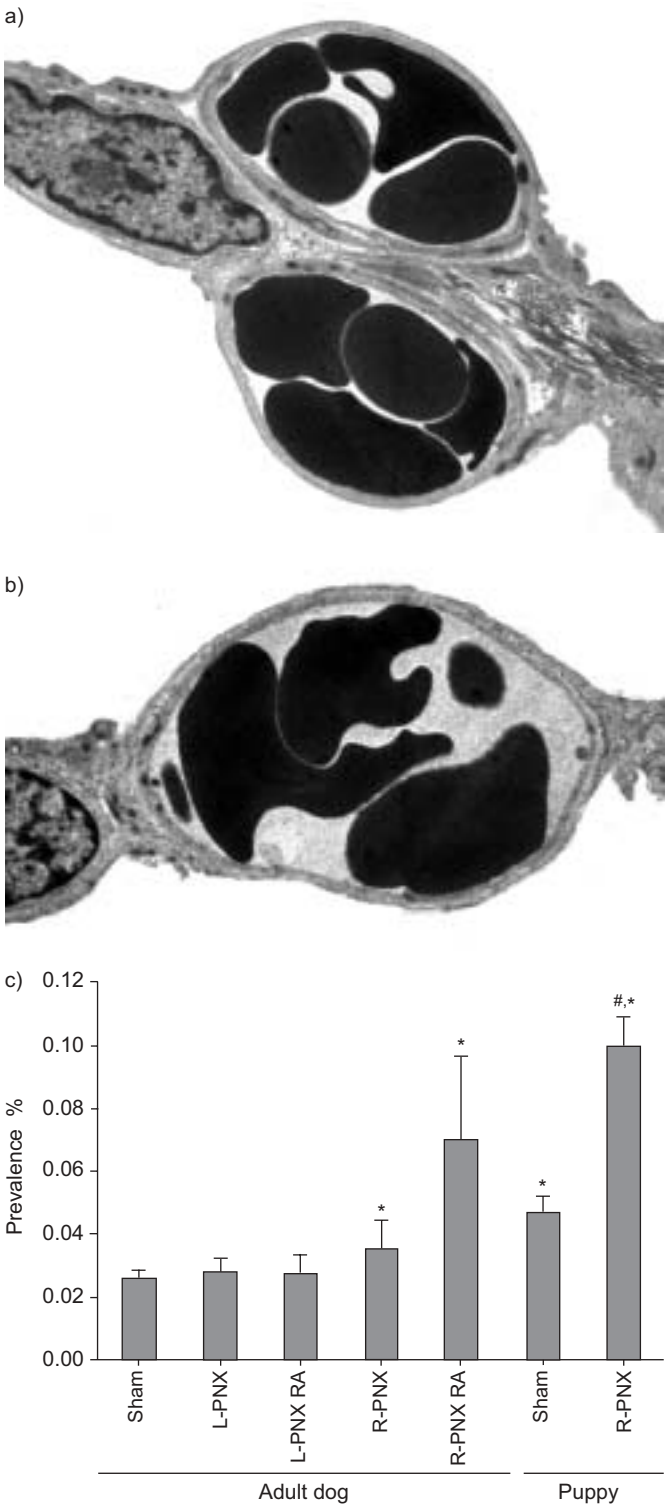

FIGURE 3. Electron micrographs illustrate a) double and b) single alveolar capillary profiles. c) The bar graph shows the prevalence of double capillary profiles in the lung of adult dogs and puppies under different experimental conditions. The bars indicate mean ± SD values. Data are taken from [19, 22, 50]. Sham: normal; L-PNX: left pneumonectomy; R-PNX: right pneumonectomy; RA: pneumonectomy followed by all-*trans*-retinoic acid supplementation. *: $p<0.05$ *versus* adult Sham; #: $p<0.05$ *versus* puppy Sham.

In contrast, the extra-acinar conducting airways do not branch or proliferate post-pneumonectomy but adapt by elongation [55, 56] and dilatation [57–59], which is evident on morphological analysis. The long-term compensatory increases in airway volume and cross-sectional area lag behind the increase in parenchyma volume, leading to persistently elevated airways resistance and work of breathing [60] even as alveolar gas exchange normalises [22] >1 yr after pneumonectomy. The effects of dissociated or dysanaptic growth rates between conducting and gas exchange structure are more pronounced in dogs undergoing pneumonectomy as puppies than as adults, and imposes a mechanical limit on the function of the remaining lung that curtails the effectiveness of alveolar growth.

Quantifying lung growth by high-resolution computed tomography

High-resolution computed tomography (HRCT) is a powerful noninvasive modality for assessing temporal changes in lung structure; its main disadvantage, radiation exposure and resolution limit, continues to be improved as technology advances. By identifying interlobar fissures, HRCT can be

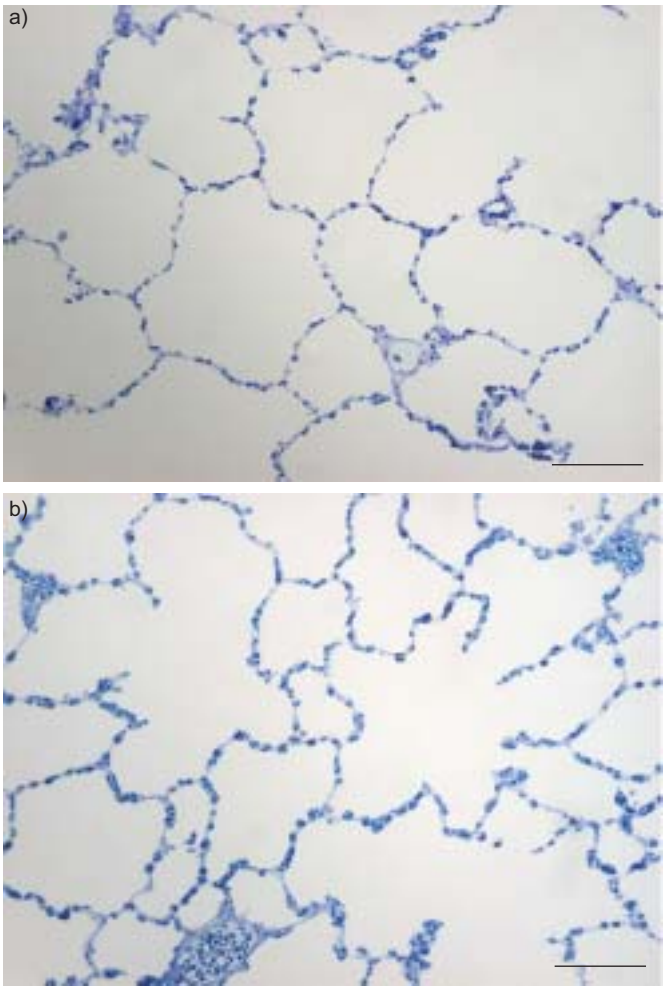

FIGURE 4. Retinoic acid supplementation following right pneumonectomy alters alveolar septal morphology in the remaining lung with higher volume density and the arithmetic thickness of alveolar septum and a reduced surface area/septal volume ratio. a) Placebo; b) retinoic acid supplementation. Scale bars = 100 μm.

used to reconstruct lobar anatomy and quantify regional morphology of the lung parenchyma and conducting structure (fig. 5). Using HRCT, the present author has shown in growing dogs following right pneumonectomy, that lengthening of the remaining airways occurs within 4 months while dilatation becomes evident later [61]. These processes exert opposing effects on airways resistance, which is inversely proportional to the fourth power of airway diameter and is directly related to airway length. Even a minimal increase in distal airway diameter can substantially reduce airflow resistance and more than offset the effect of airway lengthening. Dilatation or elongation must have been accompanied by the addition of new airway tissue or by a redistribution of existing airway tissue.

The HRCT attenuation of lung parenchyma has been used to estimate lung weight, gas volume, surface/volume ratio and airway dimensions in patients with emphysema and diffuse lung disease [62, 63]. In patients undergoing lung resection, estimates by HRCT and morphometry yield similar proportions of tissue to air in the resected lobe [64]. From the calibrated attenuation values of air-free tissue (including blood) and intrathoracic air, and after using an attenuation threshold to exclude major conducting airways and vessels, the measured attenuation value within any given region can be partitioned into fractional tissue and air volumes [65, 66]. This technique has been used to track parenchymal growth in children [67, 68] where gas volume per gram of lung tissue decreases initially after birth before increasing steadily to 17 yrs of age [68]. The present author's group has also observed by HRCT that volume density of lung tissue declines in young dogs from 6.5–12.5 months of age [34]. *In vivo*, HRCT-derived tissue volume correlates significantly with physiological estimates of gas exchange septal volume by a rebreathing method at comparable lung volumes [69] and with *post mortem* morphometric estimates of septal volume [70]; these correlations demonstrate internal consistency of independent methods. However, HRCT estimates are systematically larger than the corresponding rebreathing and morphometric estimates, probably because the so-called HRCT-derived ''tissue volume'' includes not only the volume of alveolar septa but also extra-septal tissue of conducting airways and vessels up to 1 mm in diameter and the blood within these small vessels.

After pneumonectomy, perfusion to the remaining lung doubles immediately; parenchymal growth following stabilisation of perfusion is associated with proportional increases in HRCT-derived tissue and blood volumes; physiological measurements of membrane diffusing capacity and capillary blood volume also increase proportionally [22, 69, 71]. In adult dogs, the post-pneumonectomy compensatory increase in HRCT-derived lobar tissue volume is markedly heterogeneous (fig. 6). Serial HRCT of the lungs of puppies demonstrates uniform lobar growth during post-natal maturation; however, in pneumonectomised puppies, non-uniform lobar growth develops slowly, 4–10 months after surgery; the remaining lower lobe grows at a slower rate [34]. When these animals are raised to maturity, the pattern of lobar heterogeneity is similar to that in animals pneumonectomised as adults. The differences in lobar growth rates may reflect non-uniform transmission of intrathoracic mechanical forces resulting from anatomical constraints imposed by asymmetric mediastinal structures and ligaments. These data illustrate the evolving use of HRCT to quantitatively follow slowly evolving structural responses.

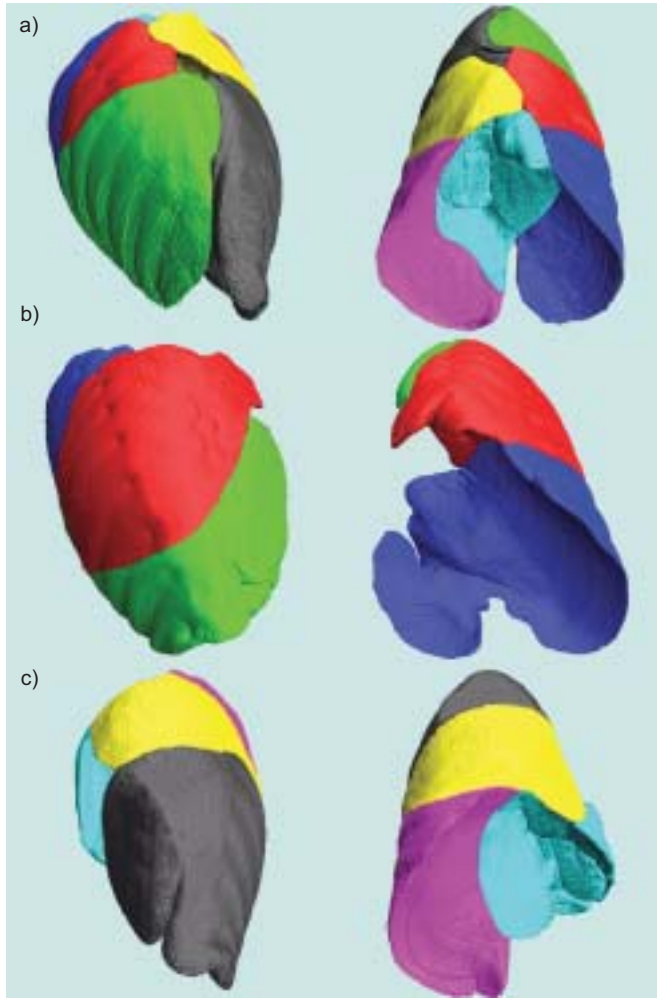

FIGURE 5. Three-dimensional high-resolution computed tomography reconstruction of a) both lungs in a normal dog (Sham), b) the left lung in a dog after undergoing right pneumonectomy (PNX), and c) the right lung in a dog after left PNX, each shown in dorsal (left-hand side) and caudal (right-hand side) views oriented by their coordinate axes. Each lobe is designated by a specific colour, as follows. Right upper: grey; right middle: yellow; right caudal: magenta; right infra-cardiac or accessory: light blue; left upper: green; left middle: red; left lower: dark blue.

CONCLUSIONS

Compensatory lung growth is defined by an absolute increase in the quantity of gas exchange tissue or conducting structure in response to injury and/or disease, leading to a positive impact on functional outcome. A robust model of compensatory lung growth is that seen following pneumonectomy, where the anatomical loss of lung units is reproducible and the remaining units are free of injury or disease. Quantifying the morphology of growth involves specific evaluation of the techniques of sampling and analysis, the adequacy of ultrastructural resolution and the selection of markers for measurement that correlate with function. Morphometric measurements should be interpreted in the context of their aggregate effects on organ architecture and physiology. The

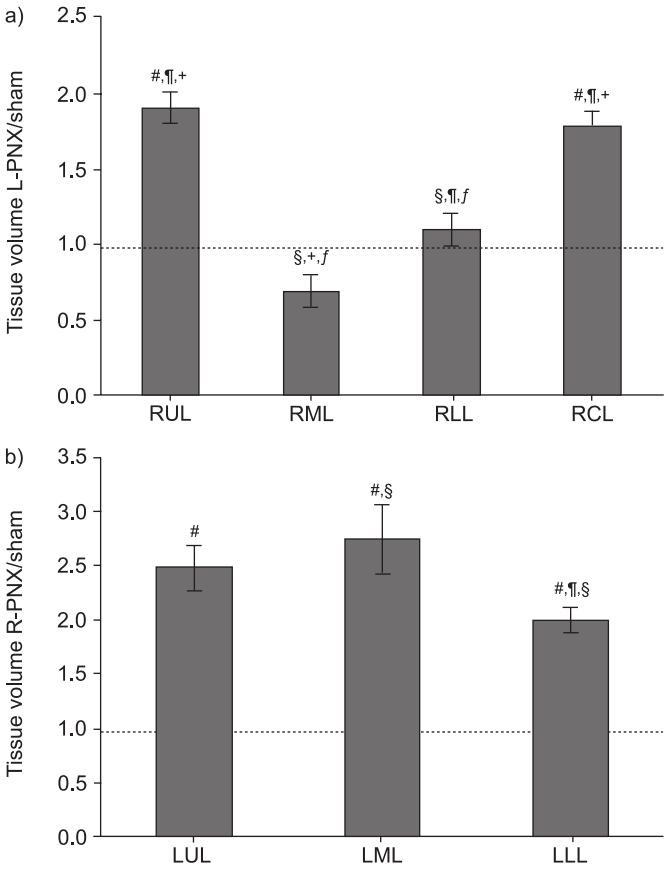

FIGURE 6. Increases of lobar tissue volume are heterogeneous in adult dogs following a) left pneumonectomy (L-PNX) or b) right pneumonectomy (R-PNX). The high-resolution computed tomography-derived tissue volume of the remaining lung is expressed as ratios to the mean value in corresponding lobes of control (Sham) lungs. Bars indicate mean ± SEM. RUL: right cranial or upper lobe; RML: right middle lobe; RLL: right caudal or lower lobe; RCL: right cardiac lobe; LUL: left cranial or upper lobe; LML: left middle lobe; LLL: left caudal or lower lobe. -----: unity (ratio of 1.0). #: $p<0.05$ *versus* 1.0; ¶: $p<0.05$ *versus* RML or LML; +: $p<0.05$ *versus* RLL or LLL; §: $p<0.05$ *versus* RUL or LUL; f: $p<0.05$ *versus* RCL. Data are taken from [70].

potential for structure–function dissociation should be recognised in any attempt to manipulate compensatory lung growth. Technical advances in high-resolution computed tomography have enabled its use in the quantitative assessment of regional lung structure as well as temporal changes in airways and gas exchange parenchyma during development and compensation. Although contrast-enhanced high-resolution !computed tomography is commonly used to evaluate regional pulmonary vascular abnormalities, the quantitative aspects of this application require further development in order to extend this noninvasive imaging modality to the assessment of vascular growth.

REFERENCES

1 American Thoracic Society. American Thoracic Society Workshop Document. Mechanisms and limits of induced postnatal lung growth. *Am J Respir Crit Care Med* 2004; 170: 319–343.

2 Cagle PT, Thurlbeck WM. Postpneumonectomy compensatory lung growth. *Am Rev Respir Dis* 1988; 138: 1314–1326.

3 Rannels DE, Rannels SR. Compensatory growth of the lung following partial pneumonectomy. *Exp Lung Res* 1988; 14: 157–182.

4 Lechner AJ, Banchero N. Lung morphometry in guinea pigs acclimated to hypoxia during growth. *Respir Physiol* 1980; 42: 155–169.

5 Johnson RL Jr, Cassidy SS, Grover RF, Schutte JE, Epstein RH. Functional capacities of lungs and thorax in beagles after prolonged residence at 3,100 m. *J Appl Physiol* 1985; 59: 1773–1782.

6 Burri PH, Weibel ER. Morphometric estimation of pulmonary diffusion capacity. II. Effect of P_{O_2} on the growing lung, adaptation of the growing rat lung to hypoxia and hyperoxia. *Respir Physiol* 1971; 11: 247–264.

7 Sekhon HS, Thurlbeck WM. Time course of lung growth following exposure to hypobaria and/or hypoxia in rats. *Respir Physiol* 1996; 105: 241–252.

8 Hsia CCW, Carlin JI, Ramanathan M, Cassidy SS, Johnson RL Jr. Estimation of diffusion limitation after pneumonectomy from carbon monoxide diffusing capacity. *Respir Physiol* 1991; 83: 11–21.

9 Hsia CCW. Recruitment of lung diffusing capacity: update of concept and application. *Chest* 2002; 122: 1774–1783.

10 Hsia CCW, Ramanathan M, Estrera AS. Recruitment of diffusing capacity with exercise in patients after pneumonectomy. *Am Rev Respir Dis* 1992; 145: 811–816.

11 Hsia CCW, Fryder-Doffey F, Stalder-Navarro V, Johnson RL Jr, Weibel ER. Structural changes underlying compensatory increase of diffusing capacity after left pneumonectomy in adult dogs. *J Clin Invest* 1993; 92: 758–764. Erratum in *J Clin Invest* 1994; 93: 913.

12 Hsia CC, Johnson RL Jr. Further examination of alveolar septal adaptation to left pneumonectomy in the adult lung. *Resp Physiol Neurobiol* 2006; 151: 167–177.

13 Fehrenbach H. Alveolar epithelial type II cell: defender of the alveolus revisited. *Respir Res* 2001; 2: 33–46.

14 Kotton DN, Ma BY, Cardoso WV, *et al.* Bone marrow-derived cells as progenitors of lung alveolar epithelium. *Development* 2001; 128: 5181–5188.

15 Ali NN, Edgar AJ, Samadikuchaksaraei A, *et al.* Derivation of type II alveolar epithelial cells from murine embryonic stem cells. *Tissue Eng* 2002; 8: 541–550.

16 Danto SI, Shannon JM, Borok Z, Zabski SM, Crandall ED. Reversible transdifferentiation of alveolar epithelial cells. *Am J Respir Cell Mol Biol* 1995; 12: 497–502.

17 Hsia CCW, Herazo LF, Fryder-Doffey F, Weibel ER. Compensatory lung growth occurs in adult dogs after right pneumonectomy. *J Clin Invest* 1994; 94: 405–412.

18 Hsia CCW, Zhou XS, Bellotto DJ, Hagler HK. Regenerative growth of respiratory bronchioles in dogs. *Am J Physiol Lung Cell Mol Physiol* 2000; 279: L136–L142.

19 Yan X, Bellotto DJ, Foster DJ, *et al.* Retinoic acid induces nonuniform alveolar septal growth after right pneumonectomy. *J Appl Physiol* 2004; 96: 1080–1089.

20 Hsia CCW, Herazo LF, Ramanathan M, Johnson RL Jr, Wagner PD. Cardiopulmonary adaptations to pneumonectomy in dogs. II. Ventilation–perfusion relationships and microvascular recruitment. *J Appl Physiol* 1993; 74: 1299–1309.

21 Hsia CCW, Herazo LF, Ramanathan M, Johnson RL Jr. Cardiopulmonary adaptations to pneumonectomy in dogs. IV. Membrane diffusing capacity and capillary blood volume. *J Appl Physiol* 1994; 77: 998–1005.

22 Takeda S, Hsia CCW, Wagner E, Ramanathan M, Estrera AS, Weibel ER. Compensatory alveolar growth normalizes gas exchange function in immature dogs after pneumonectomy. *J Appl Physiol* 1999; 86: 1301–1310.

23 Voswinckel R, Motejl V, Fehrenbach A, *et al.* Characterisation of post-pneumonectomy lung growth in adult mice. *Eur Respir J* 2004; 24: 524–532.

24 Brown LM, Malkinson AM, Rannels DE, Rannels SR. Compensatory lung growth after partial pneumonectomy enhances lung tumorigenesis induced by 3-methylcholanthrene. *Cancer Res* 1999; 59: 5089–5092.

25 Brown LM, Welch DR, Rannels SR. B16F10 melanoma cell colonization of mouse lung is enhanced by partial pneumonectomy. *Clin Exp Metastasis* 2002; 19: 369–376.

26 Foster DJ, Moe OW, Hsia CC. Upregulation of erythropoietin receptor during postnatal and postpneumonectomy lung growth. *Am J Physiol Lung Cell Mol Physiol* 2004; 287: L1107–L1115.

27 Foster DJ, Yan X, Bellotto DJ, *et al.* Expression of epidermal growth factor and surfactant proteins during postnatal and compensatory lung growth. *Am J Physiol Lung Cell Mol Physiol* 2002; 283: L981–L990.

28 Zhang Q, Moe OW, Garcia JA, Hsia CC. Regulated expression of hypoxia-inducible factors during postnatal and postpneumonectomy lung growth. *Am J Physiol Lung Cell Mol Physiol* 2006; 290: L880–L889.

29 Gil J, Bachofen H, Gehr P, Weibel ER. Alveolar volume–surface area relation in air- and saline-filled lungs fixed by vascular perfusion. *J Appl Physiol* 1979; 47: 990–1001.

30 Cruz-Orive LM, Weibel ER. Recent stereological methods for cell biology: brief survey. *Am J Physiol* 1990; 258: L148–L156.

31 Gundersen HJG, Jensen EB. The efficiency of systematic sampling in stereology and its prediction. *J Microscopy* 1987; 147: 229–263.

32 Glenny RW, Lamm WJ, Albert RK, Robertson HT. Gravity is a minor determinant of pulmonary blood flow distribution. *J Appl Physiol* 1991; 71: 620–629.

33 Glenny RW, Bernard S, Robertson HT, Hlastala MP. Gravity is an important but secondary determinant of regional pulmonary blood flow in upright primates. *J Appl Physiol* 1999; 86: 623–632.

34 Ravikumar P, Yilmaz C, Dane DM, Johnson RL Jr, Estrera AS, Hsia CCW. Developmental signals do not further accentuate non-uniform post-pneumonectomy compensatory lung growth. *J Appl Physiol* 2007; 102: 1170–1177.

35 Oldmixon EH, Suzuki S, Butler JP, Hoppin FG Jr. Perfusion dehydration fixes elastin and preserves lung air-space dimensions. *J Appl Physiol* 1985; 58: 105–113.

36 Yan X, Polo Carbayo JJ, Weibel ER, Hsia CC. Variation of lung volume after fixation when measured by immersion or Cavalieri method. *Am J Physiol Lung Cell Mol Physiol* 2003; 284: L242–L245.

37 Weibel ER. Morphometric and stereological methods in respiratory physiology, including fixation techniques. *In*: Otis AB, ed. Techniques in the Life Sciences. Respiratory Physiology. Oxford, Elsevier, 1984; pp. 1–35.

38 Weibel ER, Federspiel WJ, Fryder-Doffey F, *et al.* Morphometric model for pulmonary diffusing capacity. I. membrane diffusing capacity. *Respir Physiol* 1993; 93: 125–149.

39 Hsia CCW, Chuong CJC, Johnson RL Jr. Red cell distortion and conceptual basis of diffusing capacity estimates: a finite element analysis. *J Appl Physiol* 1997; 83: 1397–1404.

40 Okada O, Presson RG Jr, Kirk KR, Godgey PS, Capen RL, Wagner WW. Capillary perfusion patterns in single alveolar walls. *J Appl Physiol* 1992; 72: 1838–1844.

41 Frank AO, Chuong CJC, Johnson RL Jr. A finite-element model of oxygen diffusion in the pulmonary capillaries. *J Appl Physiol* 1997; 82: 2036–2044.

42 Federspiel WJ. Pulmonary diffusing capacity: implications of two-phase blood flow in capillaries. *Respir Physiol* 1989; 77: 119–134.

43 Hsia CCW, Chuong CJC, Johnson RL Jr. Critique of the conceptual basis of diffusing capacity estimates: a finite element analysis. *J Appl Physiol* 1995; 79: 1039–1047.

44 Hsia CCW, Johnson RL Jr, Shah D. Red cell distribution and the recruitment of pulmonary diffusing capacity. *J Appl Physiol* 1999; 86: 1460–1467.

45 Gehr P, Bachofen M, Weibel ER. The normal human lung: ultrastructure and morphometric estimation of diffusion capacity. *Respir Physiol* 1978; 32: 121–140.

46 Wu EY, Ramanathan M, Hsia CCW. Role of hematocrit in the recruitment of pulmonary diffusing capacity: comparison of human and dogs. *J Appl Physiol* 1996; 80: 1014–1020.

47 Dane DM, Hsia CC, Wu EY, *et al.* Splenectomy impairs diffusive oxygen transport in the lung of dogs. *J Appl Physiol* 2006; 101: 289–297.

48 Massaro GD, Massaro D. Postnatal treatment with retinoic acid increases the number of pulmonary alveoli in rats. *Am J Physiol* 1996; 270: L305–L310.

49 Tepper J, Pfeiffer J, Aldrich M, *et al.* Can retinoic acid ameliorate the physiologic and morphologic effects of elastase instillation in the rat? *Chest* 2000; 117: 242S–244S.

50 Yan X, Bellotto DJ, Dane DM, *et al.* Lack of response to all-*trans* retinoic acid supplementation in adult dogs following left pneumonectomy. *J Appl Physiol* 2005; 99: 1681–1688.

51 Kurz H, Burri PH, Djonov VG. Angiogenesis and vascular remodeling by intussusception: from form to function. *News Physiol Sci* 2003; 18: 65–70.

52 Weibel ER. Morphometric estimation of pulmonary diffusion capacity. I. Model and method. *Respir Physiol* 1970; 11: 54–75.

53 Weibel ER, Hsia CC, Ochs M. How much is there really? Why stereology is essential in lung morphometry. *J Appl Physiol* 2007; 102: 459–467.

54 Dane DM, Yan X, Tamhane RM, *et al.* Retinoic acid-induced alveolar cellular growth does not improve function after right pneumonectomy. *J Appl Physiol* 2004; 96: 1090–1096.

55 Boatman ES. A morphometric and morphological study of the lungs of rabbits after unilateral pneumonectomy. *Thorax* 1977; 32: 406–417.

56 Yee NW, Hyatt RE. Effect of left pneumonectomy on lung mechanics in rabbits. *J Appl Physiol: Respir Environ Exer Physiol* 1983; 54: 1612–1617.

57 Burri PH, Sehovic S. The adaptive response of the rat lung after bilobectomy. *Am Rev Respir Dis* 1979; 119: 769–777.
58 McBride JT. Postpneumonectomy airway growth in the ferret. *J Appl Physiol* 1985; 58: 1010–1014.
59 Kirchner KK, McBride JT. Changes in airway length after unilateral pneumonectomy in weanling ferrets. *J Appl Physiol* 1990; 68: 187–192.
60 Takeda S, Ramanathan M, Estrera AS, Hsia CCW. Postpneumonectomy alveolar growth does not normalize hemodynamic and mechanical function. *J Appl Physiol* 1999; 87: 491–497.
61 Dane DM, Johnson RL Jr, Hsia CCW. Dysanaptic growth of conducting airways after pneumonectomy assessed by CT scan. *J Appl Physiol* 2002; 93: 1235–1242.
62 Newell JD Jr, Hogg JC, Snider GL. Report of a workshop: quantitative computed tomography scanning in longitudinal studies of emphysema. *Eur Respir J* 2004; 23: 769–775.
63 Perez At, Coxson HO, Hogg JC, Gibson K, Thompson PF, Rogers RM. Use of CT morphometry to detect changes in lung weight and gas volume. *Chest* 2005; 128: 2471–2477.
64 Coxson HO, Mayo JR, Behzad H, *et al.* Measurement of lung expansion with computed tomography and comparison with quantitative histology. *J Appl Physiol* 1995; 79: 1525–1530.
65 Hyde RW, Wandtke JC, Fahey PJ, Utell MJ, Plewes DB, Goske M. Lung weight *in vivo* measured with computed tomography and rebreathing of soluble gases. *J Appl Physiol* 1989; 67: 166–173.
66 Wandtke JC, Hyde RW, Fahey PJ, *et al.* Measurement of lung gas volume and regional density by computed tomography in dogs. *Invest Radiol* 1986; 21: 108–117.
67 de Jong PA, Nakano Y, Lequin MH, *et al.* Estimation of lung growth using computed tomography. *Eur Respir J* 2003; 22: 235–238.
68 de Jong PA, Long FR, Wong JC, *et al.* Computed tomographic estimation of lung dimensions throughout the growth period. *Eur Respir J* 2006; 27: 261–267.
69 Takeda S, Wu EY, Epstein RH, Estrera AS, Hsia CCW. *In vivo* assessment of changes in air and tissue volumes after pneumonectomy. *J Appl Physiol* 1997; 82: 1340–1348.
70 Ravikumar P, Yilmaz C, Dane DM, Johnson RL Jr, Estrera AS, Hsia CC. Regional lung growth following pneumonectomy assessed by computed tomography. *J Appl Physiol* 2004; 97: 1567–1574.
71 Takeda S, Ramanathan M, Wu EY, Estrera AS, Hsia CCW. Temporal course of gas exchange and mechanical compensation after right pneumonectomy in immature dogs. *J Appl Physiol* 1996; 80: 1304–1312.